JOURNAL OF MATERIALS SCIENCE 26 (1991) 4054–4061

Dynamic studies of zirconia crystallization

G. T. MAMOTT*, P. BARNES, S. E. TARLING
Industrial Materials Group, Department of Crystallography, Birkbeck College, Malet Street, London WC1E 7HX, UK

S. L. JONES, C. J. NORMAN
Alcan Chemicals Ltd, Chalfont Park, Gerrards Cross, Buckinghamshire, SL9 0QB, UK

Zirconium hydroxide is a precursor material of zirconia. Variations in both chemical and physical properties of this precursor affect the properties of the final product. One of these variations is that of the pH of the liquid in contact with the final hydroxide precipitate. We show here, using advanced dynamic diffraction techniques, how pH affects the kinetic aspects of synthesis: In particular we investigate the effect of pH on the temperature of onset of crystallization, the rate of crystallization and crystal growth during calcination, as well as the temperature and rate of transformation, on cooling, of the tetragonal to monoclinic form of zirconia.

1. Introduction

Zirconia is an important ceramic powder which finds application in widely differing fields, such as ceramic colours, engineering ceramics, gemstones, piezoelectrics, ion exchangers and solid electrolytes. The properties required of the powder depend upon the application for which each individual batch is destined. Whilst for some applications the material obtained directly from naturally occurring baddeleyite with its variation in properties may be good enough, it is essential to control the material properties very closely for other purposes such as piezoelectrics and electrolytes [1].

Zirconium hydroxide is a key precursor of zirconia during chemical preparation. It has long been appreciated that the final properties of the powder are affected by the preparation conditions for the hydroxide though such links have been established on the basis of cause and effect rather than any dynamic characterization of the synthesis process. For example, Torralvo *et al.* [2] and Zaitsev *et al.* [3] have varied the zirconium salts used to obtain the hydroxide, while Gimblett *et al.* [4], Rijnten [5] and Wright *et al.* [6] have varied the precipitating agent employed to produce the hydroxide; the effect of pH has been investigated to some extent by Davis [7], Mamott and co-workers [8, 9], Saito *et al.* [10], Srinivasan and co-workers [11, 12], and Tau *et al.* [13], have investigated the effect of varying the rate of base addition.

Our work has concentrated on one particular aspect of the preparation condition/property relationship, namely how changing the pH of the liquid surrounding the zirconium hydroxide precipitate affects dynamic parameters of the synthesis process, such as the onset temperature and growth kinetics for both the crystallization and tetragonal to monoclinic conversion stages.

2. Chemistry and structure

The preparation of zirconium hydroxides usually involves precipitation from a zirconium salt solution by means of base addition or the reaction of a slurry of an insoluble zirconium salt with a base [14].

There are two main structural units thought to be associated with zirconium hydroxide, their occurrences depending on the preparation route followed. One of these is the tetramer and the other, which is related to the tetramer, is a zig-zag chain of Zr atoms joined by double hydroxy-bridges. The tetramer occurs in the solid $ZrOCl_2 \cdot 8H_2O$ structure [15]. This tetramer unit has been found to be very stable, and subsequent work [16–18] has shown that it remains intact as a complex ion in solution during hydrolysis of zirconium chloride. Mak [17] indicates that the Zr atoms are connected by hydroxo-bridges whereas the terminal oxygens belong to water molecules of hydration (Fig. 1a). Clearfield [19] proposes polymerization by olation between tetramer units. Olation describes the formation of hydroxo-bridges as a result of hydrolysis. The tetramer has sixteen sites at which such condensation may occur, so polymeric growth can proceed easily in many different directions. During slow polymerization the tetramers combine so as to initially form a regular two dimensional sheet by means of olation reactions (Fig. 1b). Subsequent oxolation between the sheets to eliminate half of the hydroxo group oxygens produces the three-dimensional fluorite structure. When polymerization is rapid, there is insufficient time for this to occur in a regular fashion and so, polymerization is more random in nature. Thus a sudden increase in pH due to rapid addition of base will provide the necessary excess OH^- ions, leading to rapid polymerization of an essentially amorphous zirconium hydroxide [19]: Fig. 1c illustrates these ideas for both rapid and slow

*Present address: Department of Earth Sciences, Cambridge University, Downing Street, Cambridge, UK.

0022–2461/91 $03.00 + .12

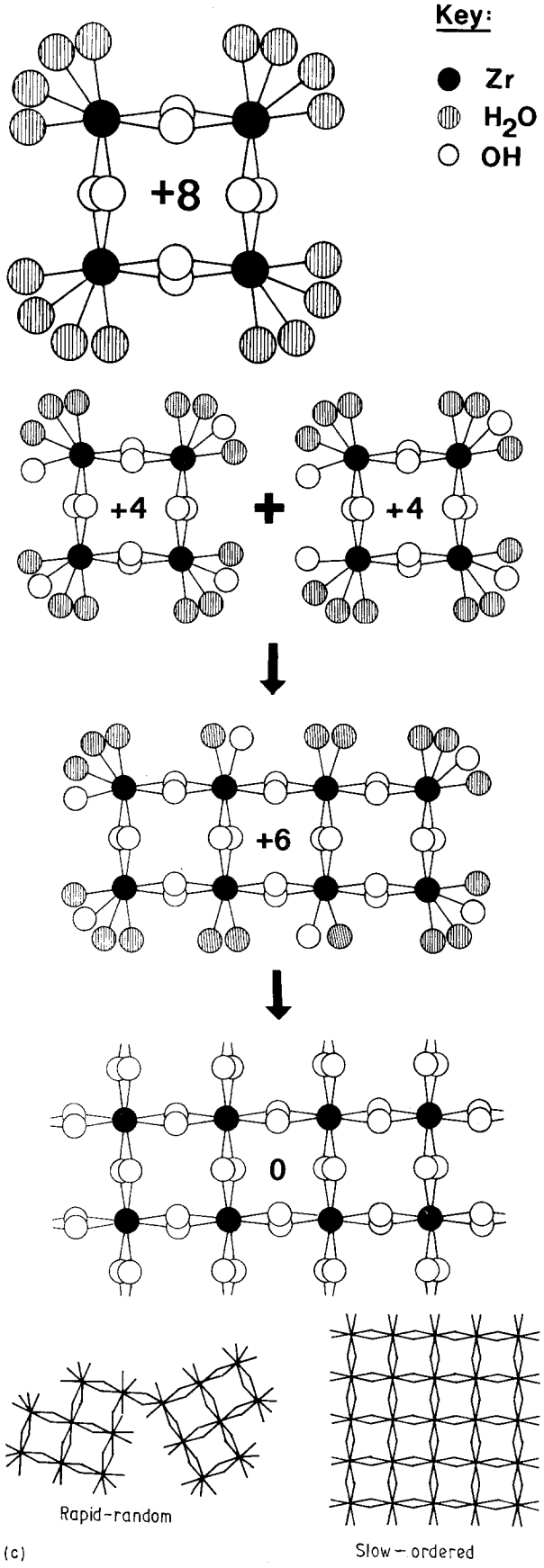

Figure 1 (a) Tetrameric structural unit associated with zirconium oxychloride [17] (the key applies to all figures); (b) schematic representation of the tetramer combination sequence; (c) schematic representation of the consequences of rapid and slow addition of base upon the structure of the resultant material [19]. The charge per unit is indicated in (a) and (b).

precipitation scenarios. Thus we can begin to envisage ways in which the preparative conditions might affect the properties of the subsequent oxide: the pH of the solution used during hydroxide precipitation directly influences the rate of polymerization and therefore the degree of localized order within the hydroxide units. The more ordered of these regions become potential nucleation sites for formation of crystalline oxide on dehydration. Thus, during calcination the rate of crystallization will reflect the pH used in the hydroxide preparation. In addition to the rate, the limit of crystallization, which can be substantially less than 100%, is found to vary with both the pH factor [8, 9] and temperature [20]. This is considered to be due to localized order which may exist to a greater or lesser extent within the amorphous material. In other words, within some areas of the material the random polymerization may well have left units favourably oriented such that they will crystallize very easily at the temperatures involved. However, other units require a considerably higher input of energy, i.e., higher operating temperatures, for them to be re-oriented in directions which will enable them to be crystallized. Fig. 2 illustrates how this might occur.

It is instructive to review the question of the structural unit. While there are no hard data concerning the hydroxide, structural studies on the oxychloride [15, 16, 18], crystalline basic sulphates [21, 22] and all three phases of the oxide [23–25] reveal striking similarities. In particular, the tetramer in the oxychloride can be seen as being closely related to the fluorite structure of the cubic phase, with the tetragonal and monoclinic forms representing the effects of distortions [26].

Basic zirconium sulphates [14] are an example of insoluble Zr salts from which zirconium hydroxide can be made. For example, the recently reported structure of $Zr_{18}O_4(OH)_{38.8}(SO_4)_{12.6}\cdot 33H_2O$ [22] shows that it consists of folded sheets of Zr atoms linked by three types of bridging oxygens. These are the double and triple-bridge hydroxo group and quadruple bridge oxide ions. In this particular structure the sulphate groups lie on the perimeter of the molecule. The zirconium atoms within the structure are shown to have either 8-fold or 7-fold coordination, once again showing that a close relationship exists with post-calcination tetragonal/cubic and monoclinic lattices of zirconia (Fig. 3a, b). Some simpler basic zirconium sulphate structures consist of chains of $Zr(OH)_2$ groups connected by bridging [21] sulphate groups.

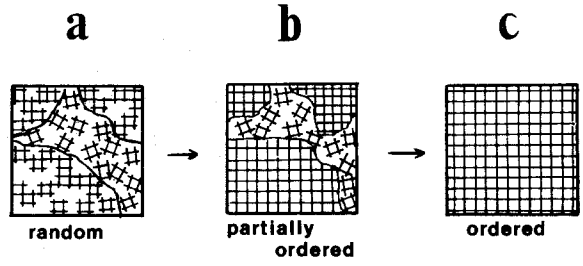

Figure 2 Sequence of events thought to give rise to limited crystallization unless further energy input is supplied: (a) Randomly oriented starting material, with some areas showing alignment; (b) material after heating. The areas previously aligned are now crystalline. Other areas are still disordered (amorphous); (c) further heat input leads to completion of crystallization.

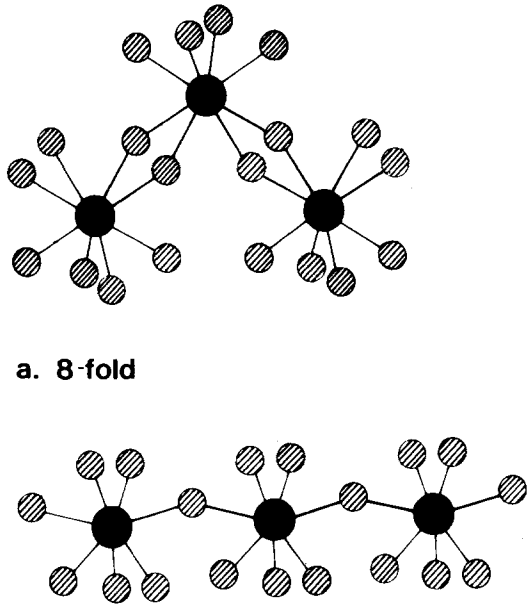

a. 8-fold

b. 7-fold

Figure 3 Coordination arrangements for zirconium atoms within the complex basic zirconium sulphate structure [22] for: (a) 8-fold coordination related to tetragonal/cubic zirconia; (b) 7-fold coordination related to monoclinic zirconia.

3. Experimental procedure

Our main investigative method, dynamic X-ray powder diffraction, has enabled us to observe in detail key parts of the synthesis process as they actually occur, during both the calcination of the zirconium hydroxide and the tetragonal to monoclinic conversion on cooling. In this study the initial sample preparation work has been carried out at Alcan Chemicals Ltd, while the dynamic X-ray diffraction techniques were implemented at the Industrial Materials Group (Department of Crystallography, Birkbeck College, London) and on Station 9.7 of the Synchrotron Radiation Source at Daresbury Laboratory.

3.1. Samples and sample preparation

The different zirconium hydroxide powders used have been prepared by varying the pH at the end of the neutralization reaction. The pH covers a narrow range of values (8.1–9.8) and the work described here covers the extremes of this range.

All samples have been pressed into circular discs of dimensions suitable for the respective sample holders (2 mm depth × 22 mm diameter for Birkbeck equipment; 0.5 mm depth × 7 mm diameter for the Daresbury work).

Scanning electron micrographs of the powders used have shown that particles are approximately *equi*-dimensional, thus minimizing any preferred orientation problems.

3.2. Dynamic X-ray diffraction

At Birkbeck a standard Siemens D-500 powder diffractometer with specially designed theta-circle, high temperature rotating sample stage and furnace, and a position sensitive detector has been used for all laboratory-based experiments [8]. An anti-scatter device within the furnace and a Pb shield positioned just ahead of the position sensitive detector maintain a favourable signal:noise ratio over the required 2θ range.

At the Daresbury Laboratory Synchrotron Radiation Source the dynamic diffraction work was carried out on Station 9.7, situated on the hard Wiggler beam line. A controllable Linkam TH1500 furnace provides the high temperature sample environment and data are collected in transmission geometry using a high purity germanium (ORTEC) solid state detector with a multi-channel analyser. Further details of the set-up are described elsewhere [27, 28].

3.3. Data collection and analysis

Preliminary work has shown that in the laboratory, with CuK_α radiation, the essential data can be collected by covering a 2θ range of 20 to 65°. This range includes the first two broad scattering bands from the amorphous hydroxide, the main low index peaks of the tetragonal phase [(1 1 1), (0 0 2), (2 0 0), (2 0 2), (2 2 0), (1 1 3), (1 3 1), (2 2 2)] and most of the monoclinic peaks. Similarly, the energy-dispersive patterns at Daresbury provide the equivalent information over an energy range of 20 to 50 keV, when the fixed scattering angle 2θ is set at 10°.

Further preliminary work has shown that no significant changes take place in the hydroxide material below 350 °C, so this has been taken as a starting temperature for data collection during heating experiments. The frequency of pattern collection has varied from experiment to experiment. In the laboratory it has usually been every 10 °C or every 10 min; with the Synchrotron experiments it has been every 3–5 min.

All patterns collected in the laboratory have been analysed using the FIT program included in the Siemens DIFFRAC-11 computer package. This involves least squares fitting of the peak profiles using a *pseudo-voigt* function. The Daresbury data have been analysed using a local variation of the program package GENIE to fit Gaussian functions to the peaks. Normalization to 100% of the weighted mean peak areas has been performed for all data shown here.

3.4. Heating/cooling regimes

The temperature–time (T–t) profiles used in all the dynamic experiments were designed to cover both standard and experimental conditions used in the production of zirconia. Two types of heating profiles have been used: isothermal and isokinetic. In the former case heating is implemented at a relatively fast rate (10–30 °C min^{-1}) up to the desired holding temperature; for isokinetic experiments a constant ramp rate (typically 10 °C min^{-1}) is maintained over the temperature range of interest. For experiments involving controlled cooling, medium to fast cooling rates of between 5 and 60 °C min^{-1} were utilized.

4. Results and discussion

The crystallization of zirconia during calcination can be quantitatively determined from the peak areas of the tetragonal pattern – the (1 1 1) peak is particularly intense and thus gives the earliest indications of onset of crystallization. Fig. 4a illustrates a typical sequence of patterns collected on the laboratory equipment during an isokinetic experiment (pH = 8.1). The pat-

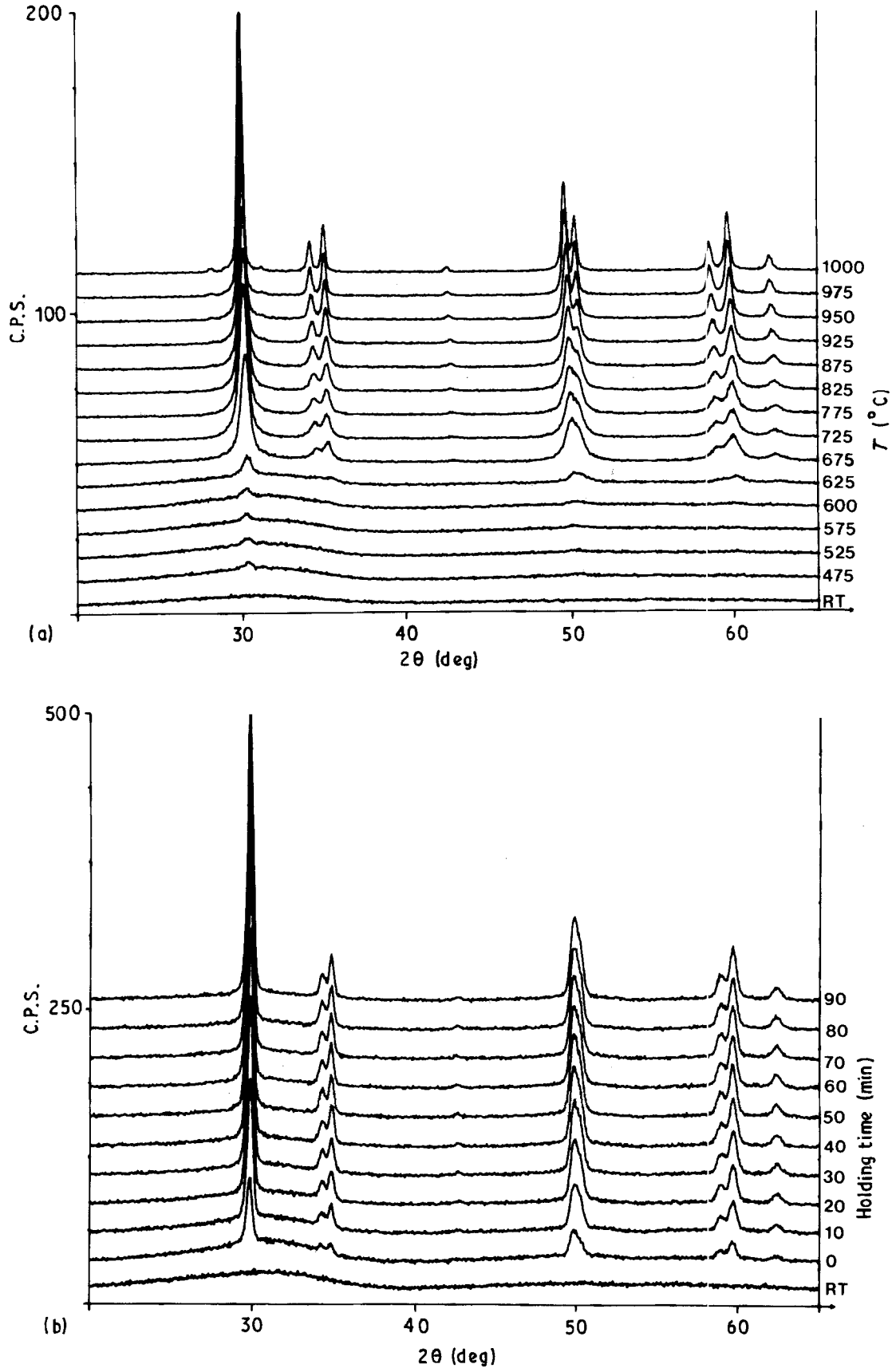

Figure 4 Two examples of time-resolved powder diffraction data sets covering the calcination of amorphous zirconium hydroxide to crystalline oxide, collected using a laboratory system with CuK_α radiation (λ = 0.1542 nm): (a) isokinetic conditions, heating rate = 1 °C min^{-1}, using hydroxide material from the 8.1 pH batch; (b) isothermal conditions, temperature held at 450 °C, using hydroxide material from the 9.8 pH batch.

tern at maximum temperature (1000 °C) represents 100% crystalline oxide. Fig. 4b shows what happens during a typical isothermal experiment for pH = 9.8 and a temperature of 450 °C. Fig. 5a shows a representative sequence of patterns, this time using the energy-dispersive Synchrotron mode, with a close-up of the subsequent phase transformation from tetragonal to monoclinic material during cooling to room temperature (Fig. 5b).

By fitting suitable functions (see above) to the diffraction peaks, the weighted mean of the peak areas for each respective phase can be determined to obtain a $\alpha(t)$ plot,where α represents the fraction of the (growing) phase at an (isothermal) temperature T (Fig. 6a). However, a particularly expressive and convenient way of comparing widely differing crystallization behaviours is to use the $\alpha(T)$ plot obtained from isokinetic diffraction data. Such plots are given in Fig. 6(b) for the two pH values (8.1, 9.8) used in this study. The two curves are similar qualitatively, consisting of the typical three-stage sigmoidal shape indicative of most crystallization processes, with shallow nucleation, rapid accelerated growth and levelling out due to impingement near the completion of transformation. However, quantitatively the slope and onset temperature vary markedly with pH, with a clear general trend of faster crystallization with higher pH: As an example one notes that the onset temperature for

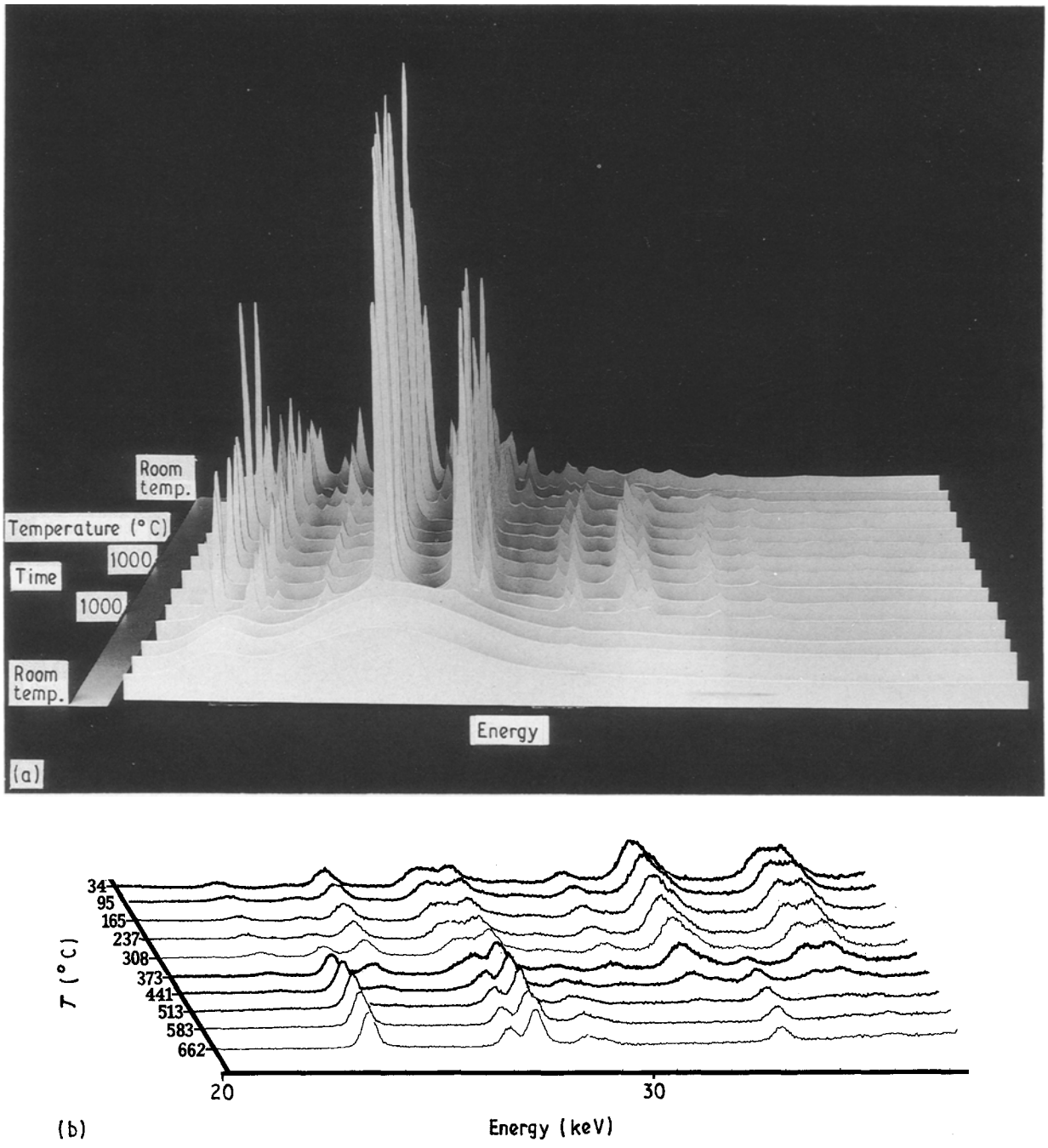

Figure 5 Dynamic diffraction data covering the calcination and conversion stages in the preparation of zirconia, obtained using the energy-dispersive diffractometer on the Daresbury Synchrotron (fixed collection angle $2\theta = 10°$): (a) A collection of energy-dispersive patterns depicting the whole sequence: heating from 20 (amorphous) to 1000 °C (tetragonal), holding at 1000 °C (tetragonal), cooling from 1000 (tetragonal) to 20 °C (monoclinic); (b) a close-up of part of the energy-dispersive patterns during cooling: the conversion of tetragonal to monoclinic oxide is very clear.

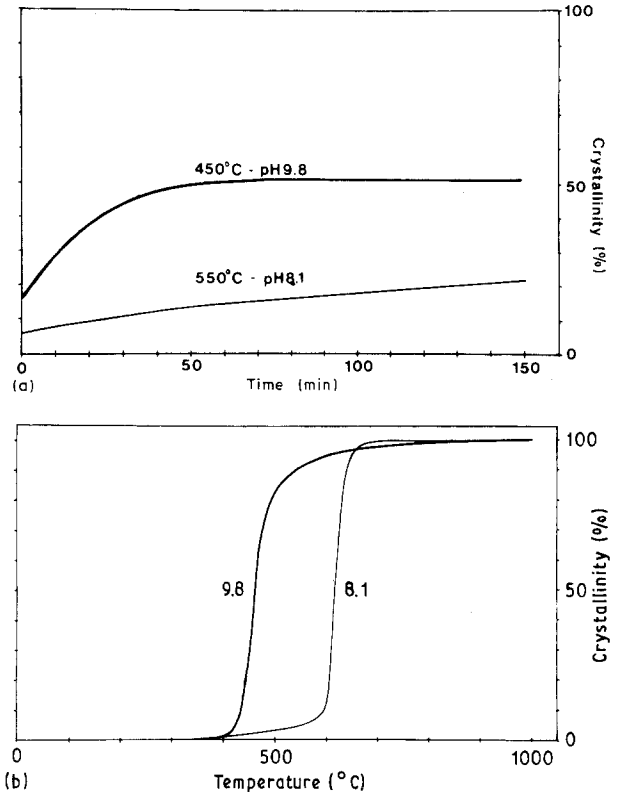

Figure 6 Crystallization curves (α-plots) for hydroxides prepared at different pH values: (a) Isothermal $\alpha(t)$ plots for two cases: holding temperature $T = 450\,^{\circ}C$, pH = 9.8, holding temperature $T = 550\,^{\circ}C$, pH = 8.1. The curves do not start at 0% due to the finite time taken to reach the holding temperature. Crystallization is much more rapid with the higher pH (9.8) batch even though the holding temperature is 100 °C lower; (b) isokinetic $\alpha(t)$ plots: Again the crystallization is much more rapid with the higher pH (9.8) batch even though the onset temperatures are comparable.

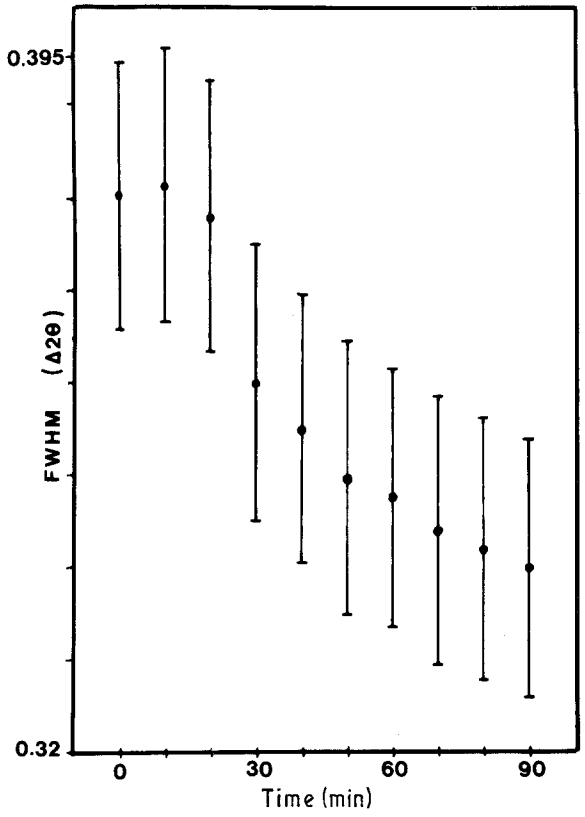

Figure 7 An example plot showing the variation of full width at half maximum (FWHM), in degrees against time during an isothermal calcination run. The reduction in FWHM indicates crystallite growth during the calcination process.

pH = 8.1 and pH = 9.8 differ by only 20 °C, while the temperature at which crystallization is complete varies by ~ 200 °C.

The question arises as to whether an increase in crystallinity is due to increasing crystallite numbers or increasing crystallite size. Neglecting strain effects, crystallite size is inversely related to the width of the diffraction peaks: a plot of peak width (full width at half maximum) from the isothermal experiments against time (Fig. 7) shows that there is indeed a significant increase in crystallite size.

Using the energy-dispersive set-up at Daresbury, two sets of experiments have been carried out: One corresponds closely to the work carried out with conventional angle dispersive diffraction in the laboratory. Here the object was to determine whether, the faster data collection possible with the Synchrotron will improve the time resolution and quality of the dynamic data obtained. In the event, the two data sets were very similar for the calcination stage, apart from an overall constant shift in apparent temperature, this being entirely attributable to the positioning of the thermocouples with respect to the sample.

The second set of energy-dispersive experiments was designed around the higher temperature, faster heating/cooling rates and superior time resolution of the Daresbury Synchrotron system. A three dimensional model has been constructed depicting the three regimes (calcination, isothermal hold, medium → fast cooling) which can now be routinely monitored with the energy-dispersive set-up (see Fig. 5a). The material remains tetragonal up to a maximum temperature and during the isothermal hold, while the tetragonal to monoclinic transformation occurs within the cooling period. Again, quantitative kinetic data ($\alpha(T)$ plots) for the tetragonal to monoclinic transformation can be extracted (Figs 8 and 9). As previously, there are marked differences apparent with different pH material when zero holding time is used, yet if the material is held at 1000 °C for 2 h, then this holding time effectively eliminates the differences due to pH, so that both materials start conversion to monoclinic within the same temperature range. In addition, the tetragonal to monoclinic transformation displays a marked dependency on cooling rates: For example, with the pH = 8.1 material the onset temperature for the conversion drops rapidly as the cooling rate increases, so much so that at a cooling rate of 30 °C min^{-1} no monoclinic material is observed; for the pH = 9.8 material the effect is less pronounced. The overall results are summarized in Table I.

5. Conclusions

It has been shown that the high temperature synthesis of zirconia from zirconium hydroxide displays distinct behavioural patterns that reflect variations in the original preparation of the hydroxide. While general relationships between preparation and final properties have been previously appreciated, we have for the first

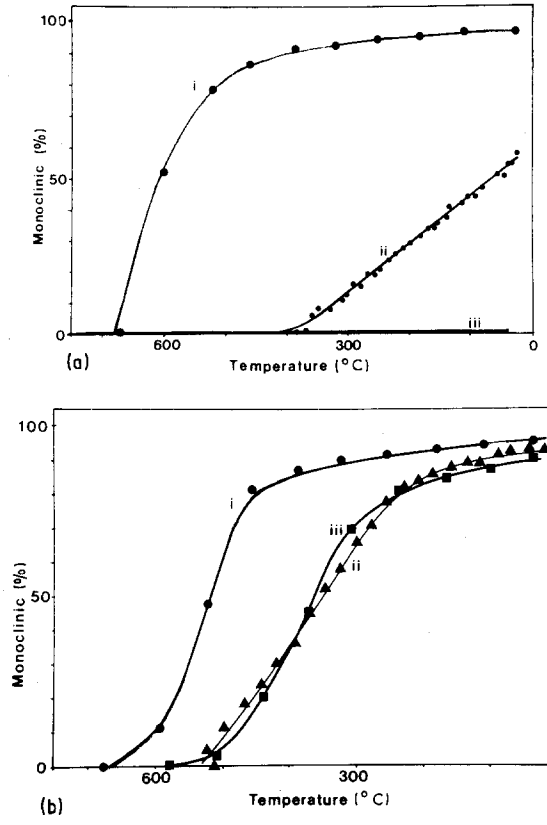

Figure 8 α-plots obtained from isokinetic cooling experiments using energy-dispersive diffraction on the Daresbury Synchrotron. The cooling from 1000 °C to room temperature covers the tetragonal to monoclinic transformation, α = 100% representing full conversion. Three temperature profiles: (i) 120 min hold at 1000 °C, cool at 30 °C min^{-1}; (ii) zero hold at 1000 °C, cool at 5 °C min^{-1}; (iii) zero hold at 1000 °C, cool at 30 °C min^{-1}; with material taken from (a) the 8.1 pH batch; and (b) the 9.8 pH batch.

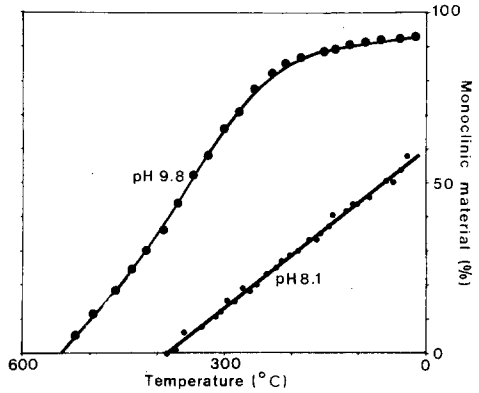

Figure 9 α-plots from isokinetic cooling experiments, as in Fig. 8, but with no holding at the maximum temperature (1000 °C): this case maximizes the difference between the 8.1 pH and 9.8 pH material.

time been able to demonstrate directly that the dynamic aspects of both calcination and tetragonal to monoclinic transformation stages are considerably affected by the pH used in the preparation of the hydroxide. The dynamic diffraction analyses, both angle-scanning in the laboratory and energy dispersive with the Synchrotron, have clearly shown that a higher pH results in faster, onset and rate of crystallization, and earlier and more complete subsequent transformation to the monoclinic phase. Furthermore, these effects become more apparent when no isothermal holding (at or above 1000 °C) is used, whereas prolonged holding will even out such differences.

These results can be interpreted in terms of a model that is consistent with the current literature on Zr coordinated structures. We assume that the tetramer unit (discussed) remains a stable entity from the starting material (oxychloride) through to the final oxide, but that the mode of joining (polymerization) of these units is the controlling factor and is pH dependent. Higher pH will promote faster polymerization and smaller but more numerous units of two/three dimensional ordered assemblages. During calcination either in vacuum or under a stream of N_2, the OH^- groups

TABLE I Summary of essential parameters obtained from dynamic diffraction experiments on the synthesis of zirconia. Results cover the two extreme pH values used in the hydroxide preparation. Temperatures quoted are not accurate on an absolute scale (errors are 5–10%), but the relative precision within each experimental set-up is high (± 5 °C, or better): (a) the calcination of amorphous zirconium hydroxide to crystalline tetragonal oxide using the laboratory powder diffraction set-up—temperatures given are for onset of crystallization, and for reaching the 50 and 90% crystallization stages; (b) the conversion from tetragonal to monoclinic oxide on cooling, using the synchrotron energy-dispersive diffraction set-up—temperatures given are for onset of conversion, and for reaching the 50 and 90% conversion stages. The final α-values indicate the degree of conversion after cooling to room temperature.

	pH = 8.1			*pH = 9.8*		
(a) Heating regime (calcination)						
onset at		410 °C			410 °C	
α = 50% at		610 °C			450 °C	
α = 90% at		650 °C			610 °C	
(b) Cooling regime (conversion)						
	5 °C min^{-1} no hold	30 °C min^{-1} + hold	30 °C min^{-1} no hold	5 °C min^{-1} no hold	30 °C min^{-1} + hold	30 °C min^{-1} no hold
onset at	384 °C	677 °C	–	532 °C	671 °C	583 °C
α = 50% at	65 °C	597 °C	–	355 °C	520 °C	360 °C
α = 90% at	–	390 °C	–	125 °C	375 °C	390 °C
final α-value at T = 20 °C:	57%	96%	0	93%	95%	90%

undergo oxolation in such a manner that these assemblages are substantially preserved to act as nuclei for crystallization of the oxide. Crystallite growth from these nuclei proceeds (as evidenced by the high temperature peak profile analysis) and thus differing rates of crystallization result from the various distributions of such nuclei as related to the pH used in the hydroxide preparation. The differences in crystallite size/growth persist to 1000 °C and are still manifested in different rates of transformation to the monoclinic form. However, such differences can be eliminated by prolonged holding at 1000 °C or higher.

Acknowledgements

The authors would like to acknowledge the help received from the following in carrying out this work: Alcan Chemicals Ltd and SERC for a CASE studentship (GTM); the London environmental/high temperature powder diffraction service at Birkbeck College for use of their laboratory facilities; SERC-Daresbury Laboratory for beam time under grant no. GR/E64633; Mr S. M. Clark, the Station Master on Station 9.7; and Dr D. Hausermann for his help in setting up the high temperature equipment at Daresbury. Further acknowledgement is due to the Photographic Unit at Birkbeck College who helped in the preparation of the illustrations for this paper.

References

1. R. STEVENS, "Zirconia and Zirconia Ceramics", Magnesium Elektron Publication No. 113. (Magnesium Elektron Ltd, UK, 1986).
2. M. J. TORRALVO, M. A. ALARIO and J. SORIA, *J. Catalysis* **86** (1984) 473.
3. L. M. ZAITSEV, V. N. ZABELIN, V. V. SAKHAROV, N. D. POLISHCHUK, V. M. KLYUCHNIKOV and I. A. APRAKSIN, *Russ. J. Inorg. Chem.* (Transl.) **17** (1972) 31.
4. G. GIMBLETT, A. A. RAHMAN and K. S. W. SING, *J. Chem. Tech. Biotechnol.* **30** (1980) 51.
5. H. T. RIJNTEN, PhD Thesis, Technological University of Delft (1971).
6. A. F. WRIGHT, S. NUNN and N. H. BRETT, in "Advances in Ceramics, Vol. 12: Science and Technology of Zirconia II", edited by N. Claussen, M. Ruhle and A. H. Heuer (The American Ceramic Society, Ohio, 1983) pp. 784–793.
7. B. H. DAVIS, *J. Amer. Ceram. Soc.* **67** (1984) C168.
8. G. T. MAMOTT, P. BARNES, S. E. TARLING, S. L. JONES and C. J. NORMAN, *Powder Diffraction* **3** (1988) 234.
9. G. T. MAMOTT, P. BARNES and S. E. TARLING, in Proceedings of the 2nd International Conference on Ceramic Powder Processing Science, Berchtesgaden, Germany edited by H. Hausner, G. L. Messing and S. Hirane (1988) (Deutsche Keramische Gelleschaft, 1990) pp. 453–460.
10. H. SAITO, H. SUZUKI and H. HAYASHI, *Nippon Kagaku Kaishi* **9** (1988) 1571.
11. R. SRINIVASAN, R. DE ANGELIS and B. H. DAVIS, *J. Mater. Res.* **1** (1986) 583.
12. R. SRINIVASAN, M. B. HARRIS, S. F. SIMPSON, R. J. DE ANGELIS and B. H. DAVIS, *ibid.* **3** (1988) 787.
13. L-M. TAU, R. SRINIVASAN, R. J. DE ANGELIS, T. PINDER and B. H. DAVIS, *ibid.* **3** (1988) 561.
14. Patent wo87/07885 Houchin, M.R., U.S.A.
15. A. CLEARFIELD and P. A. VAUGHAN, *Acta Crystallogr.* **9** (1956) 555.
16. A. CLEARFIELD, *Inorg. Chem.* **3** (1964) 146.
17. T. C. W. MAK, *Canad. J. Chem.* **46** (1968) 3491.
18. M. ABERG, *Acta Chem. Scand.* **A31** (1977) 171.
19. A. CLEARFIELD, *Rev. Pure and Appl. Chem.* **14** (1964) 91.
20. J. LIVAGE, K. DOI and C. MAZIERES, *J. Amer. Ceram. Soc.* **51** (1968) 349.
21. D. B. McWHAN and T. LUNDGUEN, *Acta Crystallogr.* **A16** (1963) 36.
22. P. J. SQUATTRITO, P. R. RUDOLPH and A. CLEARFIELD, *Inorg. Chem.* **26** (1987) 4240.
23. D. K. SMITH and H. W. NEWKIRK, *Acta Crystallogr.* **18** (1965) 983.
24. G. TEUFER, *ibid.* **15** (1962) 1187.
25. P. DUVEZ and F. ODELL, *J. Amer. Ceram. Soc.* **33** (1950) 274.
26. J. R. FRYER, J. L. HUTCHISON and R. PATERSON, *J. Colloid Interf. Sci.* **34** (1970) 238.
27. P. BARNES, S. M. CLARK, S. E. TARLING, E. POLAK, D. HAUSERMANN, C. BRENNAN, S. DOYLE, K. J. ROBERTS, J. N. SHERWOOD and R. J. CERNIK, Daresbury Laboratory Technical Memorandum, DL/SCI/TM55E, (1987).
28. J. ANWAR, P. BARNES, S. M. CLARK, E. DOORYHEE, D. HAUSERMANN, S. E. TARLING, *J. Mater. Sci. Lett.* **9** (1990) 436.

Received 3 January
and accepted 9 April 1990